Random walk model of mobility in glass formers

Grigori A. Medvedev

Phys. Rev. E **107**, 034122 — Published 14 March 2023

DOI: 10.1103/PhysRevE.107.034122

A random walk model of mobility in glass formers

Grigori A. Medvedev

Davidson School of Chemical Engineering, Purdue University

A mechanism responsible for the generic features of the mean squared displacement and the decay of the orientational autocorrelator of a molecule in a glass forming liquid is poorly understood, where such a mechanism would be critical for creating the theory of glass transition. A discrete random walk model is proposed where, instead of a straight line, a walk is along a tortuous path consisting of blocks of switchback ramps. Sub-diffusive regime, short-term dynamic heterogeneity and existence of the α- and β-relaxation processes emerge naturally from the model. The model suggests that slowing of the rate of relaxation may be due to increase in the number of the switchback ramps per block rather than due to growth of an energy barrier as typically assumed.

I. INTRODUCTION

When studying the behavior of a molecule in a condensed matter, two quantities are typically considered: the mean squared displacement (MSD), $r^2(t)=\left\langle\left[\mathbf{r}(t)-\mathbf{r}(0)\right]^2\right\rangle$, and the orientational autocorrelator, $C_1(t)=\left\langle\cos\left(\theta(t)\right)\right\rangle$. Here $\mathbf{r}(t)$ is the spatial location of a molecule at time t and $\theta(t)$ is the angle between the orientations of a chosen molecular axis at time t and at a time zero. Average $\langle\ \rangle$ is over all molecules. Orientational relaxation can also be described by higher moments of the cosine function, for example $C_2(t)=\left\langle\cos\left(2\theta(t)\right)\right\rangle=\left\langle 2\cos^2\left(\theta(t)\right)-1\right\rangle$ in two dimensions (2D); in three dimensions (3D), $C_2(t)$ is an average of the second Legendre polynomial. Typical $r^2(t)$, $C_1(t)$ and $C_2(t)$ as observed in a molecular dynamic (MD) simulation of a model system of molecular dumbbells are shown in Fig. 1.

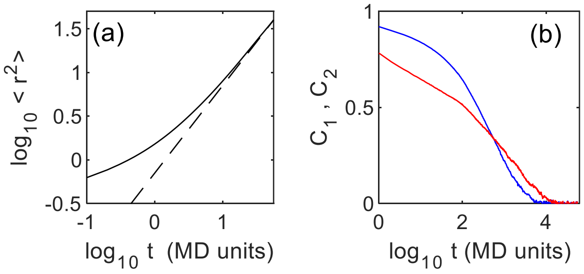

FIG. 1. Results of MD simulation of a 3D dumbbell system. (Data courtesy of J. Yungbluth) Details of the molecular potential are in Ref[1]. (a) MSD of the center-of-mass of a dumbbell, (b) rotational autocorrelators: $C_1(t)=\langle\cos\theta\rangle$ - blue (upper curve at $\log_{10}t=0$) and $C_2(t)=3\left\langle\cos^2\theta\right\rangle/2-1/2$ - red. Dashed line in (a) is the asymptote with the slope of unity.

There are several remarkable features of these dependencies. The MSD curve in Fig. 1(a) exhibits a sub-diffusive regime at intermediate times, where $\log r^2(t)$ vs $\log t$ has a slope of less than 1, and at long times a diffusive regime, where $\log r^2(t)$ vs $\log t$ has a slope of 1. (At shorter times not shown in Fig. 1(a) a ballistic regime is observed, where $\log r^2(t)$ vs $\log t$ has a slope of 2.) Asymptote for the diffusive regime in 3D, i.e., the dashed line in Fig. 1(a), is $\log r^2(t)_{asymp} = \log(6D_{trans}) + \log t$, where D_{trans} is the translational diffusion coefficient. Analysis of the MSD data for several temperatures shows that D_{trans} decreases rapidly with temperature, T.[1-3] More precisely, $D_{trans}(T)$ has an Arrhenian dependence above some material specific T_A and an even stronger super-Arrhenian dependence below T_A. As temperature decreases the sub-diffusive regime expands so that the diffusive regime is reached at increasingly longer times. At some temperature the diffusive regime cannot be reached within a practical simulation time; that temperature is the glass transition temperature, T_g. The simulated $C_1(t)$ curve in Fig. 1(b) is in a qualitative agreement with the one extracted from the analysis of the dielectric relaxation data. The autocorrelator decay is significantly broader than single exponential. Experimentally, for most materials two distinct peaks, traditionally called α- and β-relaxation processes, are seen in the spectrum.[4,5] The magnitude of the β-peak is typically an order of magnitude less than the magnitude of the α-peak.[6] There are exceptions, notably a tetramethyl tetraphenyl trisiloxane (DC704), for which virtually no β-relaxation is detected.[7] Below T_A the α-process (i.e., the slower process) exhibits a super-Arrhenian temperature dependence and the β-process (i.e., the faster process) exhibits an Arrhenian temperature dependence. An interesting feature observed in Fig. 1(b) is that the $C_2(t)$ autocorrelator initially decays more rapidly than the $C_1(t)$, but eventually begins decaying slower than the $C_1(t)$ so that the curves cross (see also Ref[8]).

The physical mechanism(s) responsible for the behavior of $r^2(t)$, $C_1(t)$ and $C_2(t)$ described above is not understood. For comparison, consider the case of a Brownian particle moving in a viscous medium. The well-known results for the $r^2(t)$, $C_1(t)$ and $C_2(t)$ functions are (in 3D)

$$r^2(t) = 6D_{trans}t \qquad C_1(t) = \exp(-2D_{rot}t) \qquad C_2(t) = \exp(-6D_{rot}t) \tag{1}$$

Here D_{rot} is the rotational diffusion coefficient related to the translational diffusion coefficient as $D_{trans} = D_{rot}l^2$ where l is on the order of the size of the Brownian particle. In contrast to the behavior depicted in Fig. 1, $r^2(t)$ in Eq. 1 has no sub-diffusive regime, $C_1(t)$ and $C_2(t)$ decay is single exponential and $C_2(t)$ always decays faster than $C_1(t)$. Glass formers are known to exhibit dynamic heterogeneity where different nanometer scale regions throughout the material have different local rates of relaxation as measured by various spectroscopic techniques.[9] An obvious idea then is to apply the Brownian particle model locally, so that the D_{trans} and corresponding D_{rot} vary from one region to another. Under that assumption, and provided the particles do not move from one region to another over the time interval of interest, Eq. 1 is replaced with

$$r^2(t) = 6\sum_n w_n D_{trans,n}t \qquad C_1(t) = \sum_n w_n \exp(-2D_{rot,n}t) \qquad C_2(t) = \sum_n w_n \exp(-6D_{rot,n}t) \tag{2}$$

Here index *n* enumerates possible values of the local diffusion coefficient $D_{trans,n}$ and w_n is the corresponding distribution, where $\sum_n w_n = 1$. While Eq. 2 does describe multi-exponential $C_1(t)$ and $C_2(t)$ functions, it still does not capture the behavior seen in Fig. 1. The $r^2(t)$ as predicted by Eq. 2 is always diffusive, where the only effect of heterogeneity is that D_{trans} in Eq. 1 is replaced by $\overline{D_{trans}} = \sum_n w_n D_{trans,n}$. Also, for every *n*, $w_n \exp(-6D_{rot,n}t)$ decays three times faster than $w_n \exp(-2D_{rot,n}t)$, so the overall $C_2(t)$ cannot cross the overall $C_1(t)$, contrary to what is seen in Fig. 1(b). If, perhaps more realistic assumption is made, that particles do not remain within a given region during the observation but move between regions with different local mobilities, then the effect of heterogeneity only weakens ultimately reverting to Eq. 1 with the effective diffusion coefficients. A Brownian particle is orders of magnitude larger than surrounding molecules, where this difference is what allows for treating the latter as an effective medium. An inescapable conclusion from the failure of Eqs. 1 and 2 to capture the behavior in Fig. 1 is that such a treatment is not appropriate for describing movement of a molecule surrounded by molecules of equal size.

II. MODEL DEVELOPMENT

A diffusive behavior described by Eq. 1 results not only from the Brownian particle model but also from a mathematically simpler model of a random walk with discrete steps. In the 1D version of the model, a walker takes steps with equal probability of moving left or right along a straight line. Position along the line is either a spatial coordinate x or an angle θ. In the former case the domain is infinite; in the latter, the periodic boundary conditions are imposed such that 2Ω steps correspond to a rotation through 2π. As stated above, Eq. 1 does not describe the behavior shown in Fig. 1. A modification of the standard random walk model is proposed, which is depicted schematically in Fig. 2. In the new model a path, along which a walker moves, is an infinite sequence of blocks, where each block comprises N_r switchback ramps of length L (i.e., it takes $L-1$ discrete steps to walk from one end of the ramp to another). The number of sites in a block is $B = (L-1)N_r$. Note that the model is strictly one-dimensional, so no physical meaning is assigned to the "displacement" in the *y*-direction in Fig. 2, which is for the clarity of the drawing only. A base diffusion coefficient for movement along the path is D_1. In order to make progress along the x-axis a walker must complete all the switchbacks within a block. Intuitively one expects the short-term behavior to be sub-diffusive and the long-term behavior to be diffusive, albeit with a diffusion coefficient smaller than D_1. The following scaling argument applies. In the asymptotic regime, a 'step' is the entire block (i.e., with the length of $L-1$) so the corresponding diffusion coefficient is given by the standard expression $D = (L-1)^2 / \tau_B$, where τ_B is the average time to traverse a block. This time is estimated to be $\tau_B = B^2 / D_1$. Thus, the asymptotic diffusion coefficient is estimated as

$$D = \frac{(L-1)^2}{\tau_B} = \frac{(L-1)^2}{B^2} D_1 = \frac{\cancel{(L-1)^2}}{\cancel{(L-1)^2} N_r^2} D_1 = \frac{D_1}{N_r^2} \tag{3}$$

In other words, the block length is canceled out and the asymptotic diffusion coefficient only depends on the number of ramps; specifically, it is inversely proportional to N_r^2.

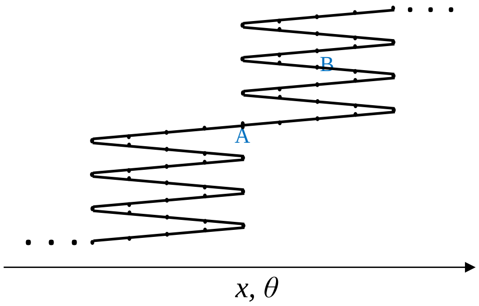

FIG. 2. Schematic of a switchback structure. The case of $N_r = 7, L = 5$ is shown. Site A is between adjacent blocks; site B is at the center of a block.

A formal treatment is possible using the characteristic function method, details of which are sketched in the Supplemental Material.[10] It involves solving an eigenproblem for the transition matrix (Hermitian of rank B), where the moments of the distribution are obtained via differentiation of the characteristic function. Although numerical differentiation is possible in principle, analytical expressions for the eigenvalues and the eigenvectors are preferred. This renders the analytical solution impractical except for the case of $L = 2, N_r = 3$, for which the mean squared displacement is obtained as

$$\left\langle x^2 \right\rangle (t) = \frac{t}{9} + \frac{8}{27} - \frac{8}{27}\left[3t+1\right]\left(-\frac{1}{2}\right)^t \tag{4}$$

where discrete time, t, is the number of steps. (See details of the derivation in the Supplemental Material.[10]) This is compared to the standard case of a random walk on a straight line where $\left\langle x^2 \right\rangle (t) = t$. As number of steps increases, Eq. 4 approaches the asymptote $\left\langle x^2 \right\rangle \square\, t/9, t >> 1$; so, the scaling result of Eq. 3 is confirmed.

For the rest of the values of L and N_r considered here, a numerical simulation of a random walk is employed. In the steady-state regime, which is of interest here, initial position of a walker is uniformly distributed within a block. Averaging is over at least 10^5 trajectories, which has proven sufficient to generate smooth $r^2(t)$, $C_1(t)$ and $C_2(t)$ curves shown below. Note that the saw-like pattern seen in the curves in Fig. 3 at short times is not noise but a consequence of the discreteness of the system.

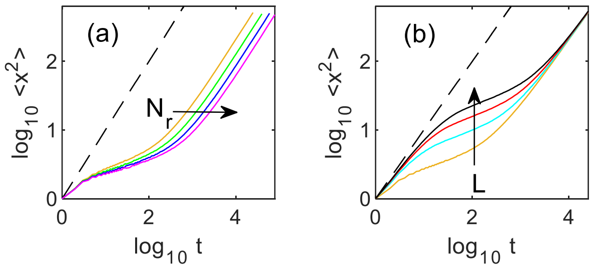

FIG. 3. MSD vs time for the switchback model; (a) effect of varying the number of ramps at fixed $L=4$ in the order indicated by the arrow: orange - $N_r=7$, green - $N_r=9$, blue - $N_r=11$, magenta - $N_r=13$; (b) effect of varying the ramp length at fixed $N_r=7$ in the order indicated by the arrow: orange - $L=4$, cyan - $L=6$, red - $L=8$, black - $L=10$. Dashed line is the standard case of a discrete random walk on a straight line $\left\langle x^2\right\rangle(t)=t$.

III. RESULTS AND DISCUSSION

Representative results of the MSD simulation are shown in Fig. 3. The shape of the curves is in qualitative agreement with the MD results in Fig. 1(a). Specifically, the sub-diffusive regime followed by the diffusive regime (i.e., the asymptote with the slope of 1) are apparent. Holding the ramp length L constant and increasing the number of ramps N_r shifts the diffusive regime to longer times, where the logarithm of the diffusion coefficient behaves as $D=N_r^{-2}D_1$ in agreement with the scaling estimate of Eq. 3. Increasing L while holding N_r constant does not affect the diffusion asymptote, but changes the shape of the sub-diffusive portion of the curve as seen in Fig. 3(b).

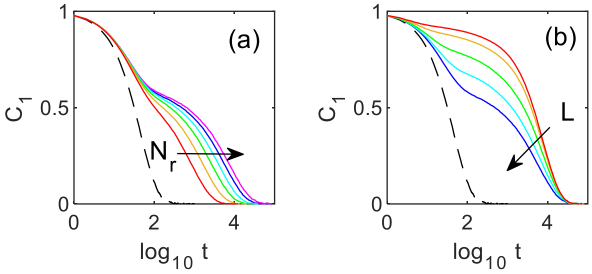

FIG. 4. Autocorrelator vs time for the switchback model for $\Omega=15$ (number of step lengths in π); (a) effect of varying the number of ramps at fixed $L=12$ in the order indicated by the arrow: red - $N_r=5$, orange - $N_r=7$, green - $N_r=9$, cyan - $N_r=11$, blue - $N_r=13$, magenta - $N_r=15$; (b) effect of varying the ramp length at fixed $N_r=13$ in the order indicated by the arrow: red - $L=5$, orange - $L=6$, green - $L=8$, cyan - $L=10$, blue - $L=12$. Dashed line is for the case of a discrete random walk on a circle for $\Omega=15$.

For orientational relaxation, the discrete steps are in terms of the angle $\theta=\pi x/\Omega$. In the simplest case of a random walk on a circle, i.e., without the switchbacks, an analytical solution is available, where the details are given in the Supplemental Material.[10] Specifically, the autocorrelators are single exponential functions $C_k(t)=\exp(-t/\tau_k)$, where $\tau_k=\ln\lambda_k^{-1}$ and $\lambda_k=\cos(k\pi/\Omega)$ for $k=1,2$. Approximate expressions, using the Taylor expansion of the cosine, are $\tau_1 \approx 2\Omega^2/\pi^2$ and $\tau_2=\tau_1/4$, which become increasingly accurate as Ω increases. The effect of increasing Ω on the base relaxation time τ_1 is equivalent to the effect of decreasing the step size on the base diffusion coefficient D_1.

In case of a random walk on the switchback structure, the value of the L/Ω ratio is consequential. If it is greater than unity, then the orientational autocorrelator can decay to zero without the walker having to leave the block where it was situated at $t=0$. If the ratio is less than unity, the walker has to visit more than a single block for the autocorrelator to fully decay. Here the focus is on the $L/\Omega\le1$ case, while holding Ω

constant, where representative examples of the $C_1(t)$ decay are shown in Fig. 4. At $L/\Omega = 1/3$ (red curve in Fig. 4(b)) the decay is nearly single exponential, but as L/Ω increases (as N_r is held constant) a shoulder develops and a two-tier decay is observed. In keeping with the traditional nomenclature, the long-term process will be called the α-relaxation and the short-term process the β-relaxation. It is apparent from Fig. 4(a) that when the ramp length L is held constant and the number of ramps N_r is increased, the α-process shifts to longer times while the β-process does not move. When the ramp length L is increased and the number of ramps N_r is held constant (i.e., in Fig. 4(b)), the relative contributions of the α- and β-processes change but there is no shifting to longer times.

The above conclusion can be made quantitative using the Prony series expansion, where a decaying function is fit to a sum of exponentials, e.g., $C_1(t) = \sum_n H_n \exp(-t/\tau_n)$. A representative example of such an expansion for the case of a well-developed two-tier decay is shown in Fig. 5(b) – blue symbols, where the spectrum is found to consists of five terms. The details of the analysis are provided in the Supplemental Material.[10] It is observed that the three terms with longer τ_n s shift with increase in N_r, while the two terms with shorter τ_n s do not. Consequentially, the three longer τ_n s are assigned to the α-relaxation process and the two shorter τ_n s are assigned to the β-relaxation process. Applying the analysis to the data in Fig. 4, it is obtained for the main α-peak

$$H_1^{(\alpha)} \exp\left[-\frac{t}{\tau_1^{(\alpha)}}\right] \qquad H_1^{(\alpha)} = 1.2 - 0.07\,L \qquad \tau_1^{(\alpha)} = N_r^2\,\tau_1 \tag{5}$$

and for the main β-peak

$$H_1^{(\beta)} \exp\left[-\frac{t}{\tau_1^{(\beta)}}\right] \qquad H_1^{(\beta)} = 0.04\,L - 0.1 \qquad \tau_1^{(\beta)} = L^2\,\frac{\tau_1}{250} \tag{6}$$

As stated above, $\tau_1^{(\alpha)}$ is a function of N_r but not L and $\tau_1^{(\beta)}$ is a function of L but not N_r. Also, in agreement with the scaling reasoning that led to Eq. 3, the α-relaxation time scales as N_r^2. According to Eq. 5, the spectral strength of the main α-peak does not change when N_r changes, which confirms that it is an objective feature rather than an artifact of fitting. The spectral strength of the main α-peak decreases with increase in the ramp length L whereas the spectral strength of the main β-peak increases with L. The relaxation times of the lesser α- and β-peaks qualitatively behave like the relaxation times of the corresponding main peaks.

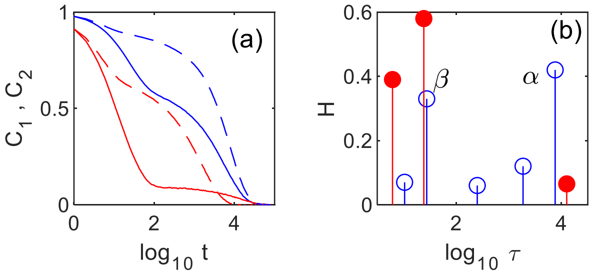

FIG. 5. (a) Orientational autocorrelators for $\Omega = 15$, $L = 6$, $N_r = 13$ case - dashed lines and $\Omega = 15$, $L = 12$, $N_r = 13$ case - solid lines; $C_1(t)$ - blue (upper) and $C_2(t)$ - red (lower) lines (b) Spectral

strength vs relaxation time for the Prony series expansion of $C_1(t)$ - blue and $C_2(t)$ - red (filled) for the $\Omega = 15$, $L = 12$, $N_r = 13$ case. Main α- and β-peaks are indicated.

Of particular interest is the effect of varying the L/Ω ratio on the relative behavior of the $C_1(t)$ and $C_2(t)$ autocorrelators. As mentioned above, in the base case of a random walk on a circle with no switchbacks $C_2(t)$ decays four times faster than $C_1(t)$. This remains approximately true in case of a switchback structure for $L \le 6$ (where $\Omega = 15$) as illustrated in Fig. 5(a) (dashed lines). In contrast, for $6 < L \le 15$ the $C_2(t)$ ultimately relaxes even slower than $C_1(t)$ as illustrated in Fig. 5(a) (solid lines). The corresponding Prony series expansions are shown in Fig. 5(b), where the expansion for $C_2(t)$ (red filled symbols) contains a long-term contribution. Analysis (see the Supplemental Material[10]) shows that the corresponding relaxation time is approximately a factor of 2 larger than the main α-relaxation time $\tau_1^{(\alpha)}$ given in Eq. 5, where it also scales as N_r^2. The reason for the difference in $C_1(t)$ vs $C_2(t)$ relaxation is easily understood. It takes a rotation through $\pm\pi/2$ angle to relax $C_2(t)$ and $\pm\pi$ angle to relax $C_1(t)$. In case of a simple diffusion on a circle, the average time required for the latter is a factor of four longer than for the former. Same mechanism applies when there are multiple switchback blocks within the $(-\pi, \pi)$ range, i.e., when the L/Ω ratio is small; only, in this case, as far as the asymptotic behavior is concerned, the 'step' is the entire block. The situation changes when the L/Ω ratio approaches $1/2$, that is when the size of a single block approaches $\pi/2$. Now the time controlling the relaxation of both $C_1(t)$ and $C_2(t)$ is the same – the time for traversing a single block. In some systems studied by the MD simulations the $C_2(t)$ relaxation is delayed as compared to the $C_1(t)$ relaxation by much greater amount than that shown in Fig. 1(b). Chong et al found that in a binary mixture of Lennard-Jones dumbbells for some dumbbell geometries the $C_2(t)$ decay was slower than $C_1(t)$ by three orders of magnitude.[11] The current model as described by Fig. 2 does not predict this. However, this is a result of a choice of a particular topology, where the model can be easily generalized. In experimental studies using the single-molecule spectroscopy, it was found that 180° flips of the embedded fluorescent probe were common even at temperatures near T_g.[12] In terms of the current model this would correspond to some of the adjacent switchback blocks being farther apart from each other along the θ-axis, so that a walker exiting one block and entering another would make a step equivalent to rotating through the angle of π. In such a version of the model the relaxation of $C_1(t)$ is accelerated and the relaxation of $C_2(t)$ is not, thereby explaining the Chong et al result.

The $C_1(t)$ and $C_2(t)$ autocorrelator decay curves shown in Figs. 4 and 5 are averages where walker's position at $t = 0$ is uniformly distributed within a block, which is consistent with the steady state assumption. However, the subsets of walkers located at $t = 0$ at different positions within a block do exhibit different relaxation responses. In Fig. 6, the autocorrelator decay for a walker initially located between adjacent blocks (i.e., at the point A in Fig. 2) is juxtaposed against that for a walker initially located in the center of a block (i.e., at the point B in Fig. 2). The responses are clearly different until the terminal stage of the relaxation. In other words, the switchback model naturally predicts some dynamic heterogeneity occurring on the time scale shorter than the main α-relaxation time. The effect is more pronounced when the block size is large. Unlike the weighted average response (i.e., dashed), the solid curves in Fig. 6 cannot be fit in their entirety by the Prony series; only the terminal stage of the relaxation in Fig. 6(a), which is independent of the initial condition, is fit by a single exponential function with the relaxation time $\tau_1^{(\alpha)}$.

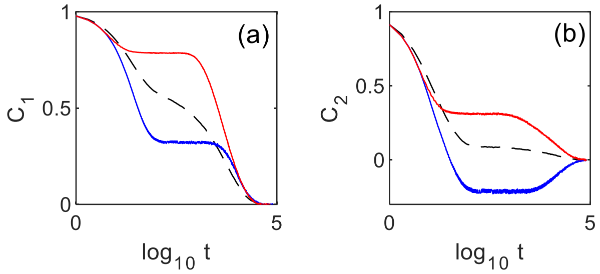

FIG. 6. Effect of initial conditions on the autocorrelator functions $C_1(t)$ and $C_2(t)$ for the $\Omega=15$, $L=12$, $N_r=13$ case. Initial position: uniformly distributed within a block – dashed, located between adjacent blocks – solid blue (lower), located in the center of a block – solid red (upper).

The switchbacks picture shown in Fig. 2 should not be interpreted as suggesting that a super-molecular structure exists in liquid. Analyzing the MSD simulation data like the one shown in Fig 1(a), one observes that the diffusive regime emerges when a molecule's displacement is on the order of the size of a molecule. In other words, the spatial scale of a block is that of a single molecule, where the switchback topology accounts for the effect of intermolecular interactions. As a discrete random walk model is not based on the realistic dynamic equations, it is not capable of predicting the thermal effects, in particular the temperature dependence of the relaxation times. However, a meaningful question may be posed as to what temperature dependence the parameters of the model must have in order to produce the experimentally observed behavior. Above we have shown that the logarithms of the α- and β-relaxation times are $\log\tau^{(\alpha)}=\log\tau_{ref}^{(\alpha)}+\log\tau_1+\log N_r^2$ and $\log\tau^{(\beta)}=\log\tau_{ref}^{(\beta)}+\log\tau_1+\log L^2$, respectively. Here $\tau_{ref}^{(\alpha)}$ and $\tau_{ref}^{(\beta)}$ are the relaxation times in some reference state and τ_1 is the base relaxation time. Any temperature dependence can be postulated for τ_1. In particular, seeing that the temperature dependence of the β-relaxation time results from the temperature dependence of the τ_1, the latter can be made Arrhenian to be in agreement with the experiments. The α-relaxation time may have an additional (i.e., beyond that of τ_1) temperature dependence provided the number of switchback ramps N_r is a function of temperature. For example, if it is assumed that each switchback ramp splits into two when temperature is decreased by ΔT then an exponential dependence of the relaxation time, and hence a linear dependence of its logarithm on T, is obtained. If the temperature decrement required to double the number of ramps is not constant but decreases as T decreases, then the temperature dependence of the relaxation time becomes even stronger, for example it can be super-Arrhenian. Thus, the current model offers an alternative mechanism for the super-Arrhenian temperature dependence, as compared to the traditional models. The traditional models rely on the growing energy barriers and the current model does not involve overcoming any energy barrier. However, it may still be possible that the free energy barrier is being overcome if it is established that the greater number of switchbacks corresponds to lower local entropy.

Although the autocorrelators in Figs. 4 and 5 need to be fit with several exponential functions, the main α- and β-relaxation processes are single exponential. Experimentally determined α- and β-processes are broad, where the spectrum for the α-process has a characteristic wedge-like shape with the longer time components dominating.[13] There is no agreed upon mechanism by which the wedge-like α-spectrum arises. A scenario can be proposed from the perspective of the switchback model. One speculates that the environments throughout the material vary. In this view, the schematic in Fig. 2 represents an ideal situation, where in equilibrium, at a given temperature and density, all blocks have equal number of switchback ramps N_r. In reality, defects i.e., shortcuts, will occur, where in a particular environment some blocks will have a number of switchback ramps less than N_r. This will result in the local relaxation time $\tau^{(\alpha)}$ being shorter than the one in the intact environment. Presumably, more drastic shortcuts occur less frequently, which would explain the experimentally observed wedge-like shape of the α-relaxation process. The idea of shortcuts also provides a plausible mechanism for the effect of large deformation, which is known to accelerate the relaxation in glassy materials.[14] It seems natural to assume that the deformation disrupts the switchback structure causing the N_r, and hence $\tau^{(\alpha)}$, to decrease. In a similar vein, in a material that is not fully equilibrated the ideal switchback structure has not yet developed, which would explain why the relaxation times in such a material are shorter than in the equilibrated one.

IV. CONCLUSIONS

In conclusion, a discrete random walk model has been proposed, where the path along which a walker moves is a sequence of blocks consisting of switchback ramps. The model predicts several features of the relaxation behavior of the glass formers, including the sub-diffusive MSD regime, emergence of the α- and β-processes, short-term dynamic heterogeneity, and the fact that in some cases the $C_2(t)$ orientational autocorrelator decays slower than the $C_1(t)$ autocorrelator. The main relaxation time of the α-process is controlled by the number of ramps in a block, N_r, and the main relaxation time of the β-processes is independent of N_r. Thus, the mechanism for the increase in the relaxation time with decrease in temperature suggested by the model is the increase in the number of the switchback ramps. This is a different perspective as compared to the models where the super-Arrhenian growth of the relaxation time is attributed to increase in an energy barrier.

ACKNOWLEDGEMENTS

The author acknowledges support from the National Science Foundation grant number 1761610-CMMI.

[1] A. P. Kerasidou, Y. Mauboussin, and V. Teboul, A simple diatomic potential that prevents crystallization in supercooled liquids simulations, Chem. Phys. **450-451**, 91 (2015).

[2] T. B. Schrøder and J. C. Dyre, Solid-like mean-square displacement in glass-forming liquids, J. Chem. Phys. **152**, 141101 (2020).

[3] J.-H. Hung, T. K. Patra, V. Meenakshisundaram, J. H. Mangalara, and D. S. Simmons, Universal localization transition accompanying glass formation: insights from efficient molecular dynamics simulations of diverse supercooled liquids, Soft Matter **15**, 1223 (2019).

[4] C. M. Roland, Relaxation Phenomena in Vitrifying Polymers and Molecular Liquids, Macromolecules **43**, 7875 (2010).

[5] A. Kudlik, S. Benkhof, T. Blochowicz, C. Tschirwitz, and E. A. Rossler, The dielectric response of simple organic glass formers, J. Mol. Struct. **479**, 201 (1999).

[6] H. Wagner and R. Richert, Spatial uniformity of the β-relaxation in D-sorbitol, J. Non·Cryst. Solids **242**, 19 (1998).

[7] T. Hecksher, D. H. Torchinsky, C. Klieber, J. A. Johnson, J. C. Dyre, and K. A. Nelson, Toward broadband mechanical spectroscopy, Proc. Natl. Acad. Sci. U.S.A. **114**, 8710 (2017).

[8] C. De Michele and D. Leporini, Viscous flow and jump dynamics in molecular supercooled liquids. II. Rotations, Phys. Rev. E **63**, 036702 (2001).
[9] M. D. Ediger, Spatially Heterogeneous Dynamics in Supercooled Liquids, Annu. Rev. Phys. Chem. **51**, 99 (2000).
[10] Supplemental Material.
[11] S.-H. Chong, A. J. Moreno, F. Sciortino, and W. Kob, Evidence for the Weak Steric Hindrance Scenario in the Supercooled-State Reorientational Dynamics, Phys. Rev. Lett. **94**, 215701 (2005).
[12] D. Bingemann, R. M. Allen, and S. W. Olesen, Single molecules reveal the dynamics of heterogeneities in a polymer at the glass transition, J. Chem. Phys. **134**, 024513 (2011).
[13] P. Lunkenheimer and A. Loidl, in *Broadband Dielectric Spectroscopy*, edited by F. Kremer, and A. Schonhals (Springer-Verlag, Berlin, Heidelberg, 2003), pp. 131.
[14] H.-N. Lee, K. Paeng, S. F. Swallen, and M. D. Ediger, Direct Measurement of Molecular Mobility in Actively Deformed Polymer Glasses, Science **323**, 231 (2009).